J Pharm Biopharm Res, 2019, 1(2): 53-60
DOI: 10.25082/JPBR.2019.02.002

RESEARCH ARTICLE

Spectroscopic and molecular docking studies on the binding mechanism of Mobic and lipase

Baosheng Liu[1*] Xu Cheng[1] Hongcai Zhang[1]

Abstract: Under simulated physiological conditions (pH=7.40), the interaction between non-steroidal anti-inflammatory drug Mobic and lipase was studied by fluorescence spectra, ultraviolet absorption spectra, circular dichroism spectra and computer simulation technique. The experimental results showed that Mobic could quench the fluorescence of lipase by static quenching, and the binding site number is about 1. According to Förster's theory of non-radiation energy transfer, the binding distance between Mobic and lipase was obtained, $r<7$ nm, which indicated that there was non-radiation energy transfer in the system. The thermodynamic parameters were obtained from van't Hoff equation, Gibbs free energy $\Delta G<0$, indicating that the reaction between them was spontaneous, $\Delta H<0$, $\Delta S>0$, indicating that hydrophobic force played a major role in the formation of Mobic and lipase complex. The results of synchronous fluorescence spectra, UV spectra and circular dichroism spectra showed that Mobic changed the conformation of lipase. The molecular docking results showed that the binding position of Mobic was close to the active center, indicating that Mobic could change the microenvironment of amino acid residues at the active center of lipase catalysis. The results of docking showed that there was hydrogen bond between Mobic and lipase, so the interaction between Mobic and lipase was driven by hydrophobic interaction and hydrogen bond.

Keywords: spectroscopy, Mobic, lipase, conformation, molecular docking, interaction

1 Introduction

Non-steroidal anti-inflammatory drugs can relieve pain and edema to play a role in the treatment of inflammation, however, patients taking non-steroidal anti-inflammatory drugs often cause gastritis, gastric ulcer, kidney and liver damage and other adverse symptoms.[1] Mobic is one of the non-steroidal anti-inflammatory drugs[2] and the structural formula is shown in Figure 1. The toxic and side effects of Mobic are much less than those of some other non-steroidal anti-inflammatory drugs (such as dotaline, ibuprofen, *etc.*). Therefore, the adverse effect of Mobic on gastrointestinal function was much smaller.[3] This drug is widely used in daily life and it is a very common drug for the treatment of rheumatoid arthritis. in addition to the treatment of inflammatory diseases, Mobic also has a good effect on relieving physical pain in patients.[4]

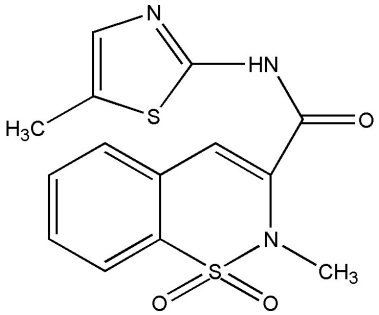

Figure 1. Chemical structure of Mobic

Lipase is a hydrolase that decomposes triacylglycerol. It is an intracellular enzyme. Its catalytic site contains a nucleophilic catalytic triad (SHD or SHE). The catalytic site is buried inside the molecule and the surface is formed by relatively hydrophobic amino acid residues. Covered by a spiral lid structure to protect the catalytic part of the triplet.[5] Human lipase is mainly secreted by pancreatic acinar cells, so it is also called pancreatic lipase, and plays a role in digesting fat in the duodenum. It plays an important role in the absorption of triglycerides in the small intestine. Hydrolyzed triglyceride is con-

Received: April 20, 2019 **Accepted:** May 10, 2019 **Published:** May 13, 2019

* **Correspondence to**: Baosheng Liu, College of Chemistry and Environmental Science, Key Laboratory of Analytical Science and Technology of Hebei Province, National Chemistry Experimental Teaching Demonstration Center, Hebei University, Baoding 071002, China; Email: lbs@hbu.edu.cn;

[1] College of Chemistry and Environmental Science, Key Laboratory of Analytical Science and Technology of Hebei Province, National Chemistry Experimental Teaching Demonstration Center, Hebei University, Baoding 071002, China

Citation: Liu B, Cheng X and Zhang H. Spectroscopic and molecular docking studies on the binding mechanism of Mobic and lipase. *J Pharm Biopharm Res*, 2019, **1**(2): 53-60.

verted into Glycerin and fatty acids are absorbed by the body[6] and play an important role in the process of digestion and absorption. Zhao Lining *et al*.[7] studied the interaction of three mercaptopropionic acid-terminated CdTe quantum dots with lipase, and proved that three mercaptopropionic acid-terminated CdTe quantum dots can cause toxic side effects on lipase; Zhang Rui *et al*.[8] studied the interaction of bisphenol A with lipase in vitro to better understand the toxicity and toxicity mechanism of bisphenol A.

In recent years, fluorescence spectroscopy has become an important means to study the mechanism of ligand-protein system. But up to now, researches on the interaction of lipase with Mobic have not been reported by a variety of spectroscopic and computer simulations. In this paper, the binding constants, binding sites, thermodynamic parameters and binding distance of the drug-protein system were obtained by spectroscopic experiments and molecular docking methods, and a series of experimental data such as binding constants, binding sites, thermodynamic parameters and binding distance were obtained. Thus, the mechanism of Mobic binding to lipase is revealed, which provides important information for more comprehensive understanding of the mechanism of drug and protein transport and harmony in human body.

2 Experimental

2.1 Apparatus

RF-5301PC fluorometer (Shimadzu, Japan); UV-3600 UV-vis spectrophotometer (Shimadzu, Japan); MOS-450/SFM300 circular dichroism (Bio-Logic, France); SYC-15$_B$super constant temperature water bath (Nanjing Sanli Electronic equipment Factory); SZ-93 automatic double Pure Water Distiller (Shanghai Yarong biochemical instrument Factory).

2.2 Materials

Porcine pancreatic lipase (PPL, purity grade inferior 99%, Sigma), reserve solution (5.0×10^{-6}mol/L); Mobic (CAS#,71125-28-7), reserve solution(4.0×10^{-4}mol/L). Tris-HCl buffer solution was used to keep the pH of the solution at 7.40, and NaCl (0.10 mol/L) solution was used to maintain the ionic strength of the solution. The water used in the experiment was secondary quartz distilled water, and the above storage solution was kept away from light at 277 K. The fluorescence signal measured in the experiment was corrected by the "internal filter effect" Equation (1):[9]

$$Fcor = Fobs \times e^{(A_{ex}+A_{em})/2} \quad (1)$$

Where F_{cor} and F_{obs} are the corrected and observed fluorescence signals, respectively, and A_{ex} and A_{em} are the absorbance values of Mobic-PPL system at excitation and emission wavelengths, respectively. The fluorescence signal used in this article was corrected.

2.3 Experiment procedure

2.3.1 Fluorescence experiment

At 298K, 310K and 318K, 1.0 mL Tris-HCl buffer solution, 2.0 mL PPL solution and different volume of Mobic solution were added to the 10.0 mL colorimetric tube at constant volume and constant temperature of 30 min. The slit width was 5 nm, λ_{ex} and the scanning fluorescence spectra were 280, 295 nm, respectively.

2.3.2 Circular dichroism measurements

At 298K, 1.0 mL Tris-HCl buffer solution, 2.0 mL PPL solution and different volume of Mobic solution were added to the 10.0 mL colorimetric tube at constant volume and constant temperature of 30 min. Circular dichroism measurements were performed with a 1.0 cm path length quartz cuvette. Each spectrum was recorded at wavelengths between 190 and 300 nm and a scan speed of 1 nm/s.

2.3.3 UV-Vis measurements

At 298 K, 1.0 mL Tris-HCl buffer solution, 2.0 mL PPL solution and different volume Mobic solution was added to the 10.0 mL colorimetric tube at constant volume and constant temperature of 30 min. The absorbance of the system was determined by using the corresponding concentration of Mobic solution as the blank reference, and the UV absorption spectrum of the system was drawn.

2.3.4 Molecular docking

The crystal structure (PDB ID: 1RP1) of PPL comes from the protein database (Protein Data Bank). The ChemDraw Pro 14.0 and ChemBio 3D Ultra 14.0 are used to draw the Mobic structure, and the energy minimization of the three-dimensional structure is carried out. AutoDock 4.2.6 was used to study the molecular docking of Mobic and PPL, and genetic algorithm was used to calculate the binding conformation of Mobic and PPL.[10]

3 Results and discussion

3.1 Fluorescence quenching mechanism studies of Mobic-PPL system

The fluorescence effect of protein is produced by the chromophore of Trp, Tyr and Phe residues. The Trp and Tyr residues in protein are excited together at 280 nm wavelength, while at 295 nm wavelength, only Trp

residue is excited.[11] Figure 2 showed the fluorescence spectra of the interaction between Mobic and PPL (at λ_{ex}=295 nm, the fluorescence spectra of Mobic and PPL are similar, but the fluorescence intensity was low). Figure 2 showed that the fluorescence peak of PPL at 343 nm quenched and the emission peak had a blue shift with the increase of Mobic concentration, indicating that the Mobic-PPL system interacted and formed a stable complex.[12]

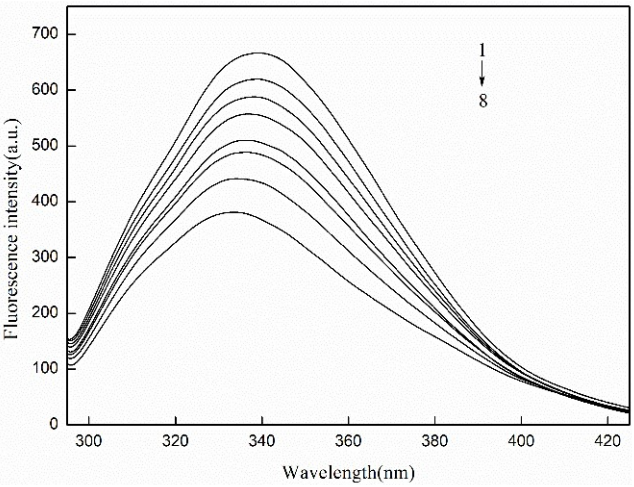

Figure 2. Fluorescence emission spectra of Mobic-PPL system (T=310 K, λ_{ex} = 280 nm), C_{PPL}=1.0×10^{-6} mol/L, 1∼8 C_{Mobic}=(0, 0.1, 0.2, 0.5, 1.0, 2.0, 3.0, 4.0)×10^{-5} mol/L

The Stern-Volmer[13] equation was shown below, through which the quenching constant K_{sv} and the quenching rate constant k_q: can be calculated by using the fluorescence signal data obtained from the experiment:

$$F_0/F = 1 + k_q\tau_0[L] = 1 + K_{SV}[L] \qquad (2)$$

Where F_0 and F represent the fluorescence signals in the absence and presence of quencher, respectively. τ_0 is the average lifetime of fluorescence without quencher, which is about 10^{-8} s. K_{sv} is the Stern-Volmer quenching constant. k_q is the bimolecular quenching constant, and[?] is the concentration of Mobic. If the quenching mechanism of the binding system is single, then the relationship curve between F_0/F and [L] is linearly correlated.[14] The Stern-Volmer equation curve of Mobic-PPL system was shown in Figure 3. From Figure 3, it could be seen that the relative fluorescence intensityF_0/F of PPL and the concentration of quenching agent Mobic showed a good linear relationship, and the linear correlation coefficient is more than 0.99. It reflected the existence of a single quenching mechanism.

The results were shown in Table 1. The results showed that the k_q values at different temperatures are larger than

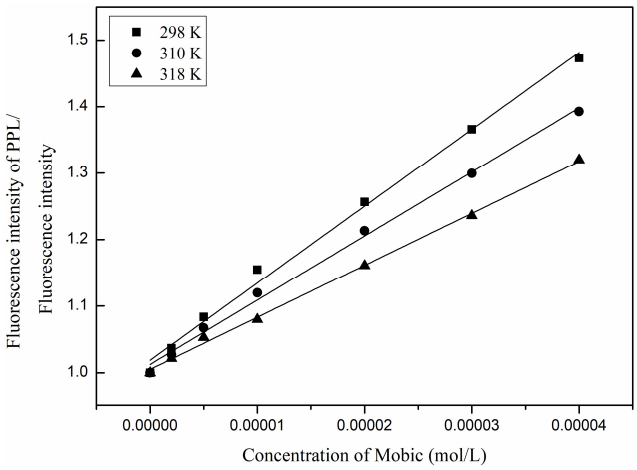

Figure 3. Stern-Volmer plots for the quenching of PPL by Mobic at different temperatures, C_{PPL} = 1.0×10^{-6} mol/L, C_{Mobic} = 0∼4.0×10^{-5} mol/L

the maximum diffusion collision quenching constant of 2×10^{10}L/mol·s[15] for biomolecules by various quenching agents. At the same time, it could be seen from the data in Table 1 that with the increase of temperature, k_q of Mobic-PPL system and K_{sv}'s are decreased. The results showed that the quenching mode of Mobic-PPL system was static quenching.

For static quenching, the Equation (3)[16] is generally used to calculate the binding constant K_a and the number of binding sites n:

$$\lg\left(\frac{F_0 - F}{F}\right) = n\lg K_a + n\lg\left\{[L] - n\frac{F_0 - F}{F_0}[B_t]\right\} \qquad (3)$$

[Bt] represents the concentration of PPL, and the results were shown in Table 1. From Table 1, n≈ 1 at the experimental temperature indicates that there is only one high affinity binding site[17] for Mobic to bind to PPL, that is, Mobic formed a 1:1 complex with PPL.The binding constant K_a of Mobic to PPL decreased with the increased of temperature, which further proved that the fluorescence quenching type of Mobic-PPL system was static quenching. Figure 4 showed the participation of Tyr residues and Trp residues of PPL in Mobic-PPL system.The results showed that when λ_{ex}=280 nm and λ_{ex}=295 nm, the quenching curve of Mobic-PPL system was separated. This indicates that both Tyr residues and Trp residues in PPL participated in the reaction. However, the slope of the quenching curve of Mobic-PPL system at λ_{ex}=295 nm was obviously smaller than that of the binding system at λ_{ex}=280 nm, which indicated that the fluorescence quenching degree of PPL was stronger at λ_{ex}=280 nm.

Table 1. Quenching reactive parameters of Mobic-PPL system at different temperatures

λ_{ex} (nm)	T/(K)	K_{sv} (L/mol·s)	k_q (L/mol)	r_1	K_a (L/mol)	n	r_2
	298	1.86×10^4	1.86×10^{12}	0.9977	2.08×10^4	1.1	0.9962
$\lambda_{ex=}280$	310	1.61×10^4	1.61×10^{12}	0.9934	1.70×10^4	1.08	0.9969
	318	1.34×10^4	1.34×10^{12}	0.9926	1.33×10^4	0.96	0.9951
	298	1.51×10^4	1.51×10^{12}	0.9961	1.47×10^4	1.01	0.9941
$\lambda_{ex=}295$	310	1.27×10^4	1.27×10^{12}	0.9963	1.22×10^4	1.12	0.9969
	318	0.99×10^4	0.99×10^{12}	0.9933	0.99×10^4	0.96	0.9911

r1 is the linear relative coefficient of F0/F~[L];

r2 is the linear relative coefficient of lg[(F0-F)/F0]~lg{[L]-n[Bt](F0-F)/F0}

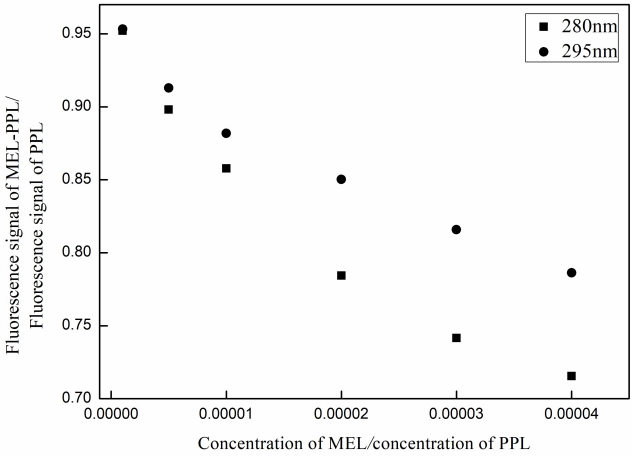

Figure 4. Relative fluorescence curves of the interaction between Mobic and PPL (T = 310 K), C_{PPL}=1.0×10^{-6} mol/L, C_{Mobic}=(0.1, 0.5, 1.0, 2.0, 3.0, 4.0)×10^{-5} mol/L

3.2 Type of interaction force of Mobic-PPL system

The thermodynamic parameters of Mobic-PPL system were calculated according to van't Hoff equation,[18] and the calculated results were shown in Table 2.

$$R\ln K = \Delta S - \Delta H/T \quad (4)$$

$$\Delta G = -RT\ln K = \Delta H - T\Delta S \quad (5)$$

Where R is a gas constant (ΔH and ΔS with a value of about 8.314), Mobic and PPL can be calculated by a linear relationship between the natural logarithm ($\ln K_a$) of the binding constant and the reciprocal (1/T) of the temperature. The results were shown in Table 2. It can be seen from Table 2 that $\Delta G<0$ indicated that the binding reaction between Mobic and PPL was spontaneous, and $\Delta H<0$ indicated that the formation of Mobic-PPL complex was exothermic. The arrangement of water molecules creates a more random configuration around drugs and proteins in a more orderly manner. Therefore, $\Delta S>0$ is usually used as evidence of hydrophobic interaction between drug molecules and protein molecules.[19,20] Based on this, the hydrophobic interaction between Mobic and PPL can be judged.

3.3 Circular dichroism spectra studies of Mobic-PPL system

As one of the well-known biophysical techniques, circular dichroism spectrum (CD) is usually used to clarify the secondary structure of proteins. In the CD spectrum, the far ultraviolet region (180 nm) mainly shows the α-helix, β-fold and irregular crimping of the protein.[21] The peaks at the left and right sides of the 208 nm and 222 nm are characteristic peaks of α-helix. The change of α-helix content can be obtained by using the following formulas:[22]

$$K_{\alpha-Helix}(\%) = \frac{-N_{MRE} - 4000}{33000 - 4000} \times 100 \quad (6)$$

The N_{MRE} is the molar ellipticity at 200 nm; the number 4000 is the N_{MRE} value of β-fold and random curl at 200 nm; and the number 33000 is the N_{MRE}value of pure α-helix at 200 nm.

$$N_{MRE} = \frac{I_{CD}}{10C_P nl} \quad (7)$$

In the equation, n is the total number of amino acids in PPL, about 450, l is the light diameter of the sample cell (cm), C_p is the concentration of protein, and I_{CD} is the intensity of CD peak. The circular dichroism spectroscopy of Mobic-PPL system was shown in Figure 5. When the molar ratio of PPL to Mobic are 1:0, 1: 10 and 1: 20, the content of α-helix structure of PPL molecules decreased from 17.65% to 4.24%. The intensity of the

Table 2. The thermodynamic parameters of Mobic-PPL at different temperatures

System	T/(K)	K_a /(L/mol)	ΔH/(kJ/mol)	ΔS/(J/mol·K)	ΔG/(kJ/mol)
λ_{ex}=280 nm	298	2.08×10^4	-17.17	25.04	-24.63
	310	1.70×10^4		25.61	-25.11
	318	1.33×10^4		24.95	-25.08

negative peaks decreases gradually and without obvious change in position and shape of the peaks. It can be concluded that the interaction between Mobic and PPL made the α-helix structure of PPL loose and changed the protein secondary structure, leading to quenching of the PPL fluorescence. But α-helical structure was still dominant.

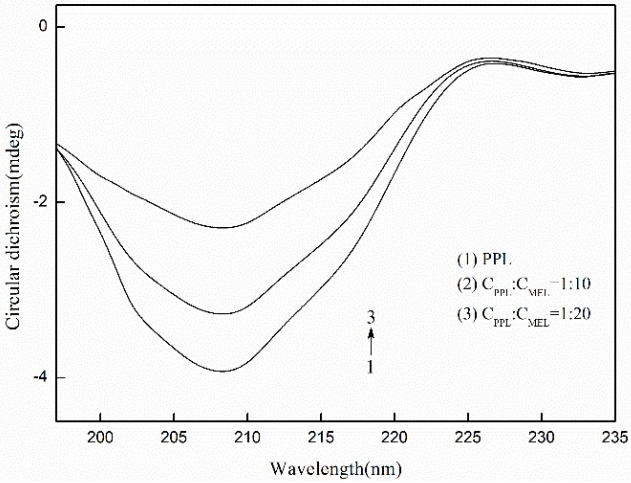

Figure 5. The circular dichroism spectra of Mobic-PPL system (T=298 K), C_{PPL} = 1.0×10^{-6} mol/L; C_{Mobic} = (0, 1.0, 2.0) $\times10^{-5}$ mol/L

3.4 UV-vis absorption spectra studies of Mobic-PPL system

UV-vis absorption spectra can be used to explore the structural changes of proteins and to study the formation of protein-ligand complexes.[23] Figure 6 was an absorption spectrum of the Mobic-PPL system. From the Figure 6, it can be seen that PPL has two absorption peaks, and its strong absorption peak near 208 nm reflects the frame conformation of the protein. The weak absorption peak at about 280 nm is due to aromatic amino acids (Trp, Tyr and Phe).[24] With the increases of Mobic concentration, Figure 6 showed that the intensity of the absorption peak at 208 nm decreases with the blue shift, and the absorption peak at 280 nm also decreases slightly. This result indicated that the interaction between Mobic and PPL led to the formation of new complexes, and the PPL molecule tended to fold, the hydrophobicity of PPL microenvironment was enhanced. The shift of UV-Vis absorption spectra indicated that the fluorescence quenching of PPL by Mobic was a static quenching process,[25] which was consistent with the results of fluorescence experiments.

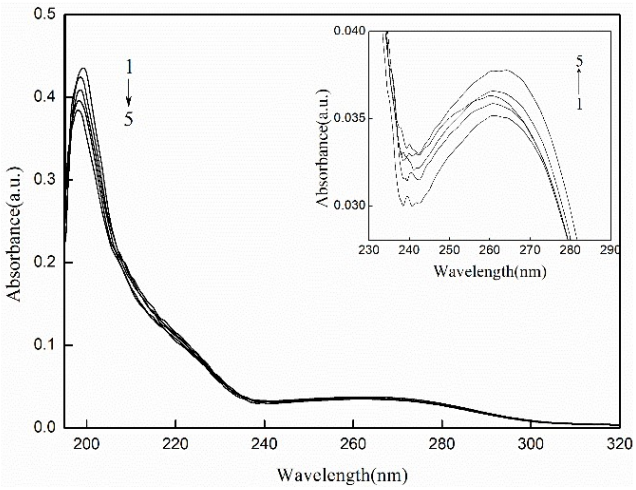

Figure 6. Absorption spectrum of Mobic-PPL system (T=298 K), C_{PPL}=1.0×10^{-6} mol/L, 1∼6: C_{Mobic}=(0, 0.1, 0.25, 0.5, 1.0)$\times10^{-5}$ mol/L

3.5 Binding distance of Mobic-PPL system

According to Frster's non-radiative energy transfer theory, when the transfer efficiency is 50%, the distance between the donor (r) and the recipient (R_0) and the energy transfer efficiency (E) can be calculated by the following formula:

$$E = 1 - F/F_0 = {R_0}^6/({R_0}^6 + r^6) \quad (8)$$

$$R_0^6 = 8.79 \times 10^{-25} K^2 \Phi N^{-4} J \quad (9)$$

$$J = \sum F(\lambda)\varepsilon(\lambda)\lambda^4\Delta\lambda / \sum F(\lambda)\Delta\lambda \quad (10)$$

In the combination system, the recipient is the PPL, donor is the Mobic, where F is the fluorescence intensity of recipient in the presence of the same concentration of

donor, K^2 is the orientation factor, Φ is the fluorescence quantum yield of the donor without the recipient, N is the refractive index at this wavelength, $F(\lambda)$ is the fluorescence intensity of the fluorescence donor at wavelength λ, and $\epsilon(\lambda)$ is the molar absorptivity of the acceptor at that wavelength. Under these experimental conditions, it is reported that K^2= 2/3, N=1.336 and Φ = 0.15.[26] J is the overlap integral between the fluorescence emission spectrum of the donor and the absorption spectrum of the recipient, as shown in Figure 7.

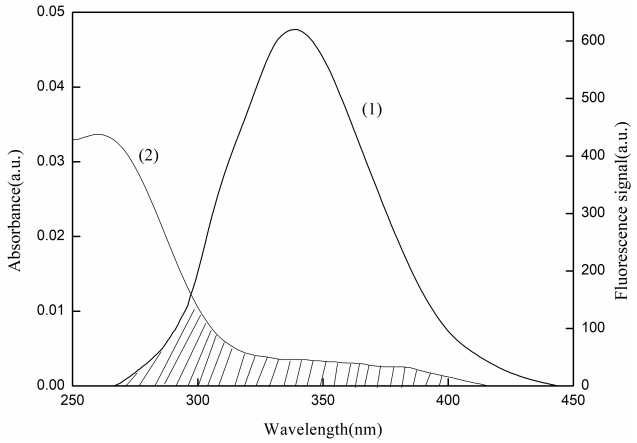

Figure 7. Fluorescence emission spectra of PPL (λ_{ex}=280 nm) (1) and UV absorption spectra of Mobic (2), (T=298 K), C_{PPL}=C_{Mobic}=1.0 × 10^{-6} mol/L

The values of J, E, R_0 and r are calculated in turn by formula and shown in Table 3. As shown in Table 3, the donor-recipient distance r<7 nm indicates a high likelihood of energy transfer from PPL to Mobic. With the increase of temperature, the distance r increases and the energy efficiency E decreases, which results in the decrease of the stability of the binary system and the decrease of the value of the binding constant K_a, which is consistent with the data obtained from the fluorescence experiment and the synchronous fluorescence experiment.

3.6 Molecular docking

Molecular docking plays an important role in exploring the interaction between ligands and receptors. In order to further determine the binding position of Mobic-PPL system and the effect of Mobic binding to PPL on ligands and receptors. In this paper, the binding model of Mobic and PPL was established by molecular docking method. By this method, the type of force and the lowest binding energy of Mobic and PPL binding system could be obtained. Figure 8(A) showed the optimal binding position of Mobic to PPL, where the Lys268 residue formed two hydrogen bonds with Mobic, with bond lengths of 2.065 $\mathring{A}$ and 1.951 $\mathring{A}$, respectively, and Mobic formed a hydrogen bond with the Ser333 residue, and its bond length is 2.148 $\mathring{A}$. These results showed that hydrogen bond played an important role in the binding of Mobic to PPL. Figure 8(B) showed a plurality of hydrophobic amino acid residues such as Phe335, Tyr267, Trp85 and Ieu275 around Mobic, further indicating that there was hydrophobic force in the binding process between Mobic and PPL. The amino acid residues such as Tyr267 and Trp85 were relatively close to the binding position of Mobic and PPL, which led to the binding could effectively quench the endogenous fluorescence of PPL, which was consistent with the conclusion of fluorescence quenching experiment. The active center of different lipases usually consists of serine (Ser) residues and histidine (His) residues, and together with aspartic acid (Asp) residues or glutamic acid (Glu) residues constitute a three meta catalytic center.[27] It could be seen from Figure 8(B) that the Mobic binding position was near the active center of the PPL. The results of molecular docking also showed that the binding of Mobic and PPL could change the microenvironment of the catalytic active center of PPL. In other words, the binding of the system might affect the catalytic activity of PPL.

The binding energy obtained from molecular docking for Mobic and PPL interaction was -25.86 kJ/mol. Whereas, the free energy change calculated from fluorescence quenching results was -25.11 kJ/mol at 310 K. This difference may be due to exclusion of the solvent in docking simulations or rigidity of the receptor other than Trp and Tyr residues.[28] The energy data obtained by docking the molecules were list in Table 4. From Table 4, it could be also seen that the electrostatic energy was very much lower than the sum of van der Waals energy, hydrogen bonding energy and desolvation free energy in the binding process of Mobic with PPL, indicating that the main interaction mode between Mobic and PPL was not electrostatic binding mode.Combined with the data of fluorescence experiments and the results of theoretical modeling, it could be seen that hydrophobic interaction and hydrogen bond were the main forces driving the combination of Mobic molecules with PPL molecules, which led to the static quenching of PPL.

4 Conclusion

In this study, Mobic reacted with PPL to form a 1:1 complex under simulated physiological conditions. The interaction of the binding system was investigated by spectroscopy and molecular docking techniques, and it was found that the binding of Mobic to PPL would change the conformation of PPL. It is of positive sig-

Table 3. Binding parameters between Mobic-PPL system at different temperatures

T/K	E (%)	J/(cm^3·L·mol^{-1})	R_0/nm	r/nm
298	3.18	5.76×10^{-15}	2.36	4.17
310	2.34	5.25×10^{-15}	2.29	4.26
318	1.84	4.62×10^{-15}	2.23	4.33

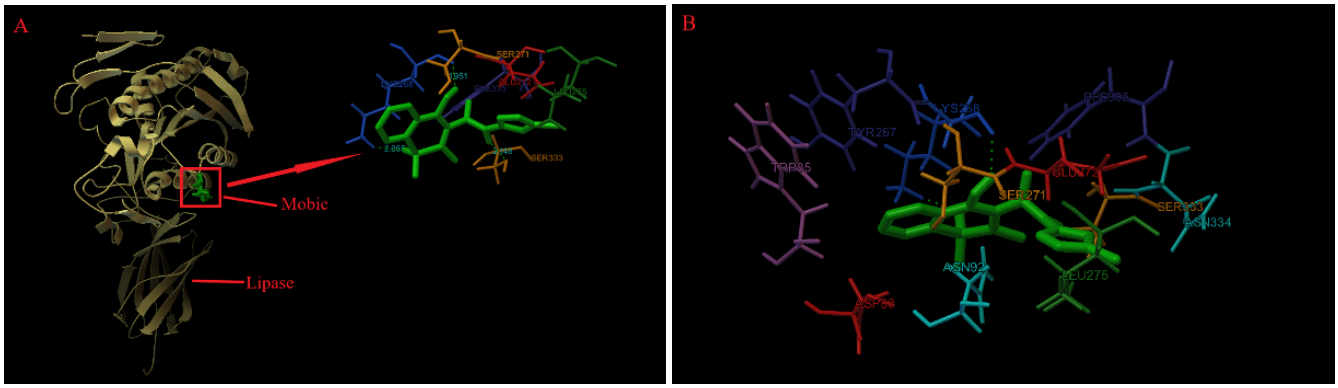

(A) (B)

Figure 8. Computation docking model of the interaction between Mobic and PPL, (A) Mobic located within the hydrophobic pocket in PPL (B) Detailed illustration of the amino acid residues lining the binding site in the Mobic and PPL cavity

Table 4. Docking energy of Mobic-PPL system (unit: kJ/mol)

Protein PDB ID	ΔG_0	ΔE_1	ΔE_2	ΔE_3
1RP1	-25.86	-29.61	-28.98	-0.63

ΔG0 is the binding energy in the binding process.

ΔE1 denotes intermolecular interaction energy, which is a sum of van der Waals energy, hydrogen bonding energy, desolvation free energy and electrostatic energy.

ΔE2 is the sum of van der Waals energy, hydrogen bonding energy and desolvation free energy.

ΔE3 is the electrostatic energy.

nificance for the study of pharmacokinetics, pharmacodynamics and toxicology of Mobic. At present, the use of spectroscopy to study the interaction between proteins and ligands is more and more popular and favored by researchers. compared with other research methods such as chromatography, this research method has the advantages of low experimental cost and short measurement period. It has a wide range of applications, so this study provides an important reference for efficient and rapid discussion of the interaction between proteins and ligands.

References

[1] Franze JA, Carvalho TF, Galieri C, *et al*. Synthesis, characterization, thermal and spectroscopic studies and bioactivity of complexes of meloxicam with some bivalent transition metals. Journal of Thermal Analysis & Calorimetry, 2017, **127**(2): 1393-1405. https://doi.org/10.1007/s10973-016-6030-5

[2] Sayen S, Carlier A, Tarpin M, *et al*. A novel copper (II) mononuclear complex with the non-steroidal anti-inflammatory drug diclofenac: structural characterization and biological activity. Journal of Inorganic Biochemistry, 2013, **120**(3): 39-43. https://doi.org/10.1016/j.jinorgbio.2012.12.002

[3] Shantiaee Y, Javaheri S, Movahhedian A, *et al*. Efficacy of preoperative ibuprofen and meloxicam on the success rate of inferior alveolar nerve block for teeth with irreversible pulpitis. International Dental Journal, 2017, **67**(2): 85-90. https://doi.org/10.1111/idj.12272

[4] Ebrahimi M, Khayamian T, Hadadzadeh H, *et al*. Spectroscopic, biological, and molecular modeling studies on the interactions of [Fe (III)-meloxicam] with G-quadruplex DNA and investigation of its release from bovine serum albumin (BSA) nanoparticles. Journal of Biomolecular Structure and Dynamics, 2015, **33**(11): 2316-2329. https://doi.org/10.1080/07391102.2014.1003195

[5] Li CY, Huang ZL, He P, *et al*. Effect of Isopropanol on Catalytic Kinetics and Molecular Spectrum of Porcine Pancreas Lipase. Chemistry & Bioengineering, 2007, **24**(9): 46-49. https://doi.org/10.3969/j.issn.1672-5425.2007.09.015

[6] Eom SH. Pancreatic Lipase Inhibitory Activity of Phlorotannins Isolated from Eisenia bicyclis. Phytotherapy

Research, 2013, **27**(1): 148-151.
https://doi.org/10.1002/ptr.4694

[7] Zhao L, Hu S, Meng Q, *et al*. The binding interaction between cadmium-based, aqueous-phase quantum dots with Candida rugosa lipase. Journal of Molecular Recognition Jmr, 2018, **31**(46): e2712.
https://doi.org/10.1002/jmr.2712

[8] Zhang R, Zhao LN and Liu RT. Deciphering the toxicity of bisphenol a to Candida rugosa lipase through spectrophotometric methods. Journal of Photochemistry & Photobiology B Biology, 2016, **163**: 40-46.
https://doi.org/10.1016/j.jphotobiol.2016.08.011

[9] Rakotoarivelo NV, Perio P, Najahi E, *et al*. Interaction between Antimalarial 2-Aryl-3H -indol-3-one Derivatives and Human Serum Albumin. The Journal of Physical Chemistry B, 2014, **118**: 13477-13485.
https://doi.org/10.1021/jp507569e

[10] Elmas G and Esra Y. Fluorescence interaction and determination of sulfathiazole with trypsin. Journal of Fluorescence, 2014, **24**(5): 1439-1445.
https://doi.org/10.1007/s10895-014-1427-7

[11] Zhang LH, Liu BS, Li ZY, *et al*. Comparative studies on the interaction of cefixime with bovine serum albumin by fluorescence quenching spectroscopy and synchronous fluorescence spectroscopy. Asian Journal of Chemistry, 2015, **30**(5): 686-692.
https://doi.org/10.1002/bio.2805

[12] Mahaki H, Memarpoor-Yazdi M, Chamani J, *et al*. Interaction between ropinirole hydrochloride and aspirin with human serum albumin as binary and ternary systems by multispectroscopic, molecular modeling and zeta potential. Journal of Luminescence, 2013, **134**(3): 758-771.
https://doi.org/10.1016/j.jlumin.2012.06.051

[13] Safarnejad A, Shaghaghi M, Dehghan G, *et al*. Binding of carvedilol to serum albumins investigated by multispectroscopic and molecular modeling methods. Journal of Luminescence,2016, **176**: 149-158.
https://doi.org/10.1016/j.jlumin.2016.02.001

[14] Jahanban-Esfahlan A, Panahi-Azar V and Sajedi S. Interaction of glutathione with bovine serum albumin: Spectroscopy and molecular docking. Food Chemistry, 2016, **202**: 426-431.
https://doi.org/10.1016/j.foodchem.2016.02.026

[15] Moeiopour F, Mohseni-Shari FS, Malaekeh-Nikouei B, *et al*. Investigation into the interaction of losartan with human serum albumin and glycated human serum albumin by spectroscopic and molecular dynamics simulation techniques: acomparison study. Chemico-Biological Interactions, 2016, **257**: 4-13.
https://doi.org/10.1016/j.cbi.2016.07.025

[16] Cao SN, Liu BS, Li ZY, *et al*. A fluorescence spectroscopic study of the interaction between glipizide and bovine serum albumin and its analytical application. Journal of Luminescence, 2014, **145**(31): 94-99.
https://doi.org/10.1016/j.jlumin.2013.07.026

[17] Amroabadi MK, Taheri-Kafrani A, Saremi LH, *et al*. Spectroscopic Studies of the interaction between alprazolam and apo-human serum transferrin as a drug carrier protein. International Journal of Biological Macromolecules, 2017, **108**: 263-271.
https://doi.org/10.1016/j.ijbiomac.2017.11.179

[18] Hu Y, Yang Y, Dai C, *et al*. Site-Selective Binding of human serum albumin by palmatine: spectroscopic approach. Biomacromolecules, 2010, **11**(1): 106-112.
https://doi.org/10.1021/bm900961e

[19] Abdus-Salam M, Rokonujjaman M, Rahman A, *et al*. Study of in Vitro Interaction of Sildenafil Citrate with Bovine Serum Albumin by Fluorescence Spectroscopy. Pharmacology & Pharmacy, 2015, **6**(2): 94-101.
https://doi.org/10.4236/pp.2015.62012

[20] Ross PD and Subramanian S. Thermodynamics of protein association reactions: forces contributing to stability. Biochemistry, 1981, **20**(11): 3096-3102.
https://doi.org/10.1021/bi00514a017

[21] Ying M, Huang FW, Ye HD, *et al*. Study on interaction between curcumin and pepsin by spectroscopic and docking methods. International Journal of Biological Macromolecules, 2015, **79**: 201-208.
https://doi.org/10.1016/j.ijbiomac.2015.04.057

[22] Bhogale A, Patel N, Mariam J, *et al*. Comprehensive studies on the interaction of copper nanoparticles with bovine serum albumin using various spectroscopies. Colloids Surf B Biointerfaces, 2014, **113**(13): 276-284.
https://doi.org/10.1016/j.colsurfb.2013.09.021

[23] Chi ZX and Liu RT. Phenotypic Characterization of the Binding of Tetracycline to Human Serum Albumin. Biomacromolecules, 2011, **12**(1): 203-209.
https://doi.org/10.1021/bm1011568

[24] Hu XX, Yu ZH and Liu RT. Spectroscopic investigations on the interactions between isopropanol and trypsin at molecular level. Spectrochimica Acta Part A: Molecular Biomolecular Spectroscopy, 2013, **108**: 50-54.
https://doi.org/10.1016/j.saa.2013.01.072

[25] Cagnardi P, Villa R, Gallo M, *et al*. Cefoperazone sodium preparation behavior after intramammary administration in healthy and infected cows. Journal of Dairy Science, 2010, **93**(9): 4105-4110.
https://doi.org/10.3168/jds.2010-3379

[26] Bertucci C and Domenici E. Reversible and covalent binding of drugs to human serum albumin: methodological approaches and physiological relevance. Current medicinal chemistry, 2002, **9**(15): 1463-1481.
https://doi.org/10.2174/0929867023369673

[27] Fan ZF, Zeng WC, Dai JL, *et al*. Interaction of Epigallocatechin-3-gallate with Porcine Pancreas Lipase. Food Science, 2013, **34**(7): 20-23.
https://doi.org/10.7506/spkx1002-6630-201307005

[28] Jana S, Dalapati S, Ghosh S, *et al*. Study of microheterogeneous environment of protein human serum albumin by an extrinsic fluorescent reporter: a spectroscopic study in combination with molecular docking and molecular dynamics simulation. Journal of Photochemistry & Photobiology B Biology, 2012, **112**(231): 48-58.
https://doi.org/10.1016/j.jphotobiol.2012.04.007